Cell, Vol. 115, 209–216, October 17, 2003, Copyright ©2003 by Cell Press

Functional siRNAs and miRNAs Exhibit Strand Bias

Anastasia Khvorova,[1,2] Angela Reynolds,[1,2] and Sumedha D. Jayasena[1,*]
[1]Amgen, Inc.
One Amgen Center Drive
Thousand Oaks, California 91320
[2]Dharmacon, Inc.
1376 Miners Drive, #101
Lafayette, Colorado 80026

Summary

Both microRNAs (miRNA) and small interfering RNAs (siRNA) share a common set of cellular proteins (Dicer and the RNA-induced silencing complex [RISC]) to elicit RNA interference. In the following work, a statistical analysis of the internal stability of published miRNA sequences in the context of miRNA precursor hairpins revealed enhanced flexibility of miRNA precursors, especially at the 5′-anti-sense (AS) terminal base pair. The same trend was observed in siRNA, with functional duplexes displaying a lower internal stability (Δ0.5 kcal/mol) at the 5′-AS end than nonfunctional duplexes. Average internal stability of siRNA molecules retrieved from plant cells after introduction of long RNA sequences also shows this characteristic thermodynamic signature. Together, these results suggest that the thermodynamic properties of siRNA play a critical role in determining the molecule's function and longevity, possibly biasing the steps involved in duplex unwinding and strand retention by RISC.

Introduction

RNA interference (RNAi) is a highly coordinated, sequence-specific mechanism involved in posttranscriptional gene regulation. During the initial steps of the process, a ribonuclease (RNase) III-like enzyme called Dicer reduces long double-stranded RNA (dsRNA) and complex hairpin precursors into small interfering RNAs (siRNAs) that degrade mRNA and microRNAs (miRNAs) that attenuate translation, respectively.

The siRNA class of molecules is comprised of 21–23 nucleotide (nt) duplexes with characteristic dinucleotide 3′ overhangs (Ambros et al., 2003; Bernstein et al., 2001). siRNAs have been shown to act as the functional intermediate in RNAi, specifically directing cleavage of complementary mRNA targets in a process that is commonly regarded to be an antiviral cellular defense mechanism (Elbashir et al., 2001a, 2001b; Fire et al., 1998; Hammond et al., 2000; Plasterk, 2002; Zamore et al., 2000). Target RNA cleavage is catalyzed by the RNA-induced silencing complex (RISC), which functions as a siRNA-directed endonuclease.

miRNAs consist of single-stranded oligoribonucleotides of roughly 20 bases in length that are processed from ~70 nt hairpin precursor RNAs (Grishok et al., 2001; Hutvágner et al., 2001; Ketting et al., 2001; Largos-Quintana et al., 2001; Lau et al., 2001; Lee and Ambros, 2001). Mature miRNAs are incorporated into a ribonucleoprotein complex that includes at least two members of the RISC, further linking siRNA and miRNA processing (Mourelatos et al., 2002). Unlike siRNAs, which regulate mRNA levels through a cleavage event, miRNAs function by attenuating translation (Hutvágner and Zamore, 2002). However, it was recently reported that a well-characterized *let-7* miRNA, which naturally directs translational attenuation, can also cleave mRNA so long as it is composed of a sequence that is completely complementary to the target (Hutvágner and Zamore, 2002). The finding that an miRNA can function as an siRNA (Doench et al., 2003; Zeng et al., 2003) indicates that the degree of sequence identity between the regulatory RNA and its target may be the key factor in determining which form of posttranscriptional gene silencing is exploited.

Several studies have shown that duplex unwinding is critical for the processing of both dsRNA and pre-miRNA hairpin precursors (Bernstein et al., 2001; Nicholson and Nicholson, 2002) and is necessary for the formation of silencing-competent (activated) RISC (RISC*), thus highlighting the importance of helicase activity in the RNAi process (Nykanen et al., 2001). In addition, recent studies in *D. melanogaster* cell lysates suggest that sequence asymmetry and strand instability in the pre-miRNA hairpin precursor or siRNA duplex may contribute to selective strand processing and entry into RISC* (Schwarz et al., 2003 [this issue of *Cell*]). Taken together, these studies hint that a correlation may exist between the thermodynamic stability of siRNAs and miRNAs and their ability to induce RNA interference.

Here, we report the results of a statistical analysis that catalogs the thermodynamic profiles of a selection of published miRNAs. Thermodynamic profiling of the miRNA precursors revealed that on average, the region corresponding to the 5′ terminus of the pre-miRNA hairpin anti-sense strand exhibited a lower internal stability relative to the rest of the precursor sequence. Analysis of a panel of siRNAs showed that similar thermodynamic characteristics were present in functional (but not nonfunctional) siRNAs as well as in siRNAs isolated after intracellular introduction of the long dsRNA. Together, these data suggest that the thermodynamic properties of siRNA molecules play a central role in determining the molecule's functionality by facilitating several steps associated with RISC in the RNAi pathway, namely duplex unwinding, strand selection, and mRNA turnover.

Results and Discussion

Biased Internal Strand Stability Is a Characteristic of miRNA Hairpin Precursors

Of the two known classes of regulatory RNAs involved in RNAi, miRNAs may be considered the natural counterparts of siRNAs. The miRNA precursors are noncoding transcripts that are predicted to form stem-loop struc-

*Correspondence: sumedhaj@amgen.com

Table 1. Free Energy Values Used for Calculating Internal Stability of RNA Duplexes (−kcal/mol)

First Nucleotide Base Pair	Second Nucleotide A	C	G	U
A-U	1.1	2.4	1.9	1.1
C-G	2.2	3.3	2.2	1.9
G-C	2.7	3.8	3.3	2.4
G-U	1.5	2.7	2.2	1.4
U-A	1.4	2.6	2.2	1.1

tures containing characteristic bulges and internal mismatches within the folded molecule. The mismatched nucleotides and bulges are predicted to destabilize the miRNA precursor and have been shown to be important features for efficient processing of the precursors to the mature miRNAs (Hutvágner and Zamore, 2002).

To look for features within the miRNA precursors that might be important for their function, a statistical analysis was performed on miRNA sequences identified in *C. elegans, D. melanogaster*, mouse, and human, using precursor hairpin and mature miRNA sequence information derived from the Sanger Institute miRNA database (http://www.sanger.ac.uk/Software/Rfam/mirna/) and published sources (Hutvágner et al., 2001; Largos-Quintana et al., 2001; Lau et al., 2001; Lee and Ambros, 2001). As mechanistic and structural differences exist in the RNAi pathways of different species, a separate analysis was performed on each group. To assess the role of destabilizing mismatches and bulges in precursor processing, internal strand thermodynamic stabilities were calculated with and without mismatch and gap penalties using energy values listed in Table 1 (Freier et al., 1986).

Figure 1 represents the *a*verage *i*nternal *s*tability *p*rofiles (AISPs) derived from 87 *H. sapiens* (Figure 1A), 73 *M. musculus* (Figure 1B), 16 *D. melanogaster* (Figure 1C), and 96 *C. elegans* (Figure 1D) miRNAs. When the average internal stability of the ~19 base miRNA precursor sequences corresponding to the mature miRNA were calculated without considering the existence of destabilizing elements (e.g., mismatches, internal bulges, and gaps, Figure 1, gray bars), the AISP values were found to be lower by an average of −1.7 kcal/mol than those computed for a collection of 19-mer RNA duplexes generated randomly (data not shown). Interestingly enough, the average internal stability profile was dramatically reduced at all positions (in all species) when energy calculations included penalties for the presence of mismatches, internal bulges, and gaps (Figure 1, black bars). On an average, AISP values measured 2.5 kcal/mol lower when energy penalties for the presence of destabilizing elements were included in calculations. In every case, the most profound effect was observed for the first base pair of the 5′ AS terminus, where the average internal stability was reduced by ~4 kcal/mol from −7.5 kcal/mol to −3.5 kcal/mol (see position 1). One possible explanation for observed low AISP at the 5′ AS termini is that the presence of destabilizing elements within the pre-miRNA hairpin precursors is required to facilitate the unwinding and eventual strand processing events that are essential for the RNAi process. This data suggests that reduced internal stability of the 5′ AS terminus, as well as the overall low stability across the region, is a conserved feature of precursor miRNA hairpins.

Functional siRNAs Have Unstable 5′ AS Termini

The analysis of miRNA precursors revealed the presence of unstable 5′ AS termini. Unlike miRNAs, siRNAs are derived from a wide range of sources including viral infections, transgene activity, or transposon hopping. Nevertheless, siRNA and miRNA precursor processing requires common, if not identical, cellular proteins. As ATP-dependent duplex unwinding is clearly a crucial step in processing of both classes of regulatory RNAs (Hutvágner and Zamore, 2002), it is reasonable to predict that the internal stability profiles of siRNA will share common features with the AISPs of miRNA and be important in determining the functionality of the molecule.

To test this prediction, a set of siRNAs (both functional and nonfunctional) were evaluated to determine whether functional siRNAs (1) exhibited a bias toward low internal strand stability, particularly at the 5′ AS terminus, and (2) possessed other thermodynamic features that correlated with functionality. To accomplish this, 37 siRNAs targeting six different genes were first evaluated in tissue culture and subsequently grouped according to their ability to downregulate the corresponding target mRNA. RNA duplexes were then divided into functional and nonfunctional categories based on the percentage of gene silencing induced by the test siRNAs. Nonfunctional siRNA were those that induced less than 70% gene silencing. In contrast, functional siRNAs were defined as those molecules that induced gene knockdown of 70% or more. Under these definitions, 16 of the 37 siRNA were found to be functional while 21 duplexes were nonfunctional.

The average internal stability profile of each member of each group was then calculated. Data sets for each group were then averaged to obtain an AISP for functional and nonfunctional siRNAs. The average internal stability profile for the 16 functional siRNAs exhibited a distinct sinusoidal pattern with a low internal strand stability of approximately −6.7 kcal/mol at the 5′ AS terminus (Figure 2A, closed squares). This trend is similar to that observed for the miRNA precursors and indicates a comparable bias toward the instability of the 5′ AS termini in both groups. In contrast, the group of 21 nonfunctional siRNAs exhibited a markedly different profile in which the average stability of the 5′ AS terminus was increased to −9 kcal/mol (Figure 2A, open squares).

Most of the siRNAs in Figure 2A were designed using $AA(N_{19})$ rule (Elbashir et al., 2002) and may have some bias in the target site selection. To eliminate any sequence bias and simultaneously determine whether the observed thermodynamic trends could be extended to a wider group of molecules, a panel of 180 independently derived siRNAs targeting every other position of an arbitrarily chosen 199 bp regions of the firefly luciferase and human cyclophilin genes were synthesized and assessed for silencing activity in tissue culture. Based on their in vivo performance, siRNAs were then divided into three groups: (1) siRNAs that induced more than 90% gene silencing (total 53), (2) siRNAs that induced less

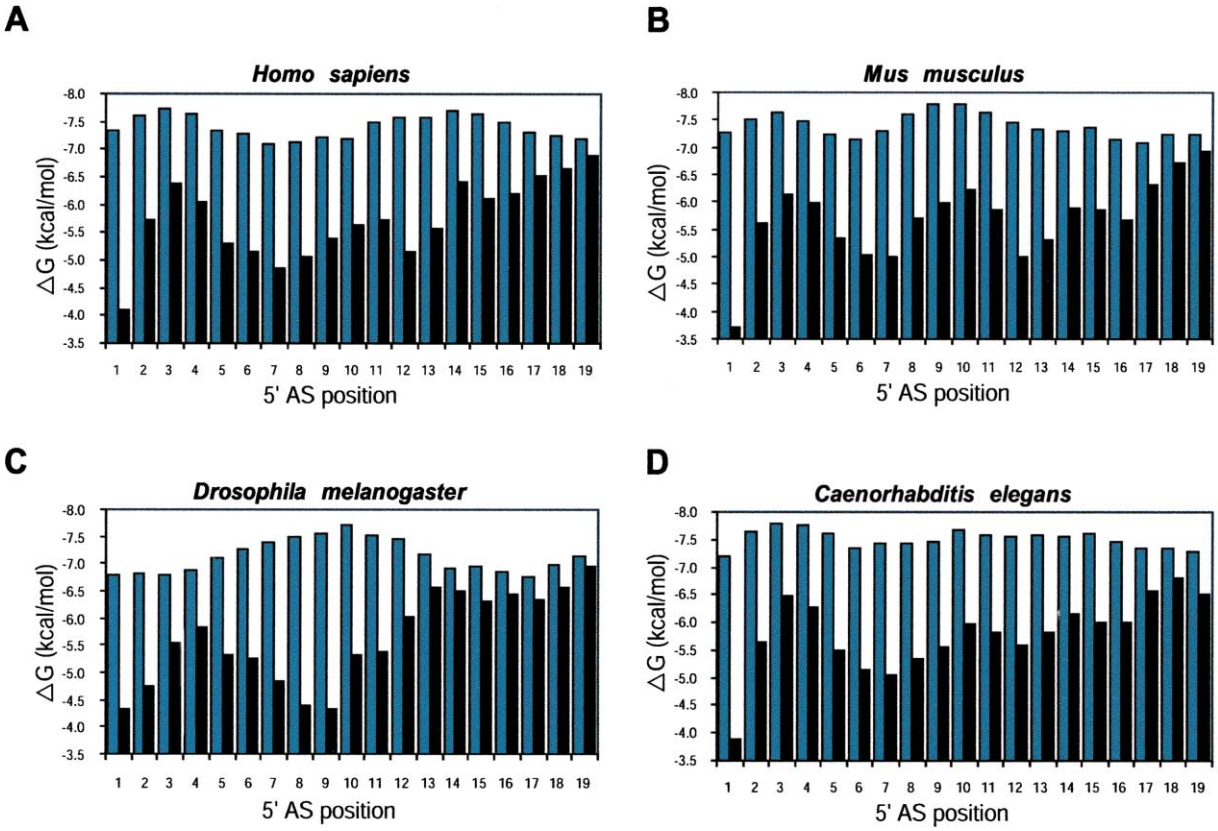

Figure 1. Calculated Average Internal Stability Profiles for Pre-miRNA Hairpin Precursors

Gray bars indicate the profile when the free energies were calculated without taking into account destabilizing elements such as mismatch and bulges or gapped nucleotides. Black bars indicate the profile when energy penalties were included for the presence of destabilizing elements for precursor sequences from *H. sapiens* (A), *M. musculus* (B), *D. melanogaster* (C), and *C. elegans* (D).

than 50% gene silencing (total 42), and (3) the remaining sequences in the collection. As was observed previously, the internal stability profiles for functional and nonfunctional subgroups appeared distinctly different, with functional siRNAs (group 1) exhibiting instability at the 5′ AS (Figure 2B). Moreover, an analysis that made comparisons between the top 10% (or 20%) with the bottom 10% (or 20%), respectively, did not significantly alter the resulting AISPs, thus demonstrating that the initial numerical boundaries used to define functional and nonfunctional subgroups can be adjusted without significantly changing the AISP profile (see Figure S1 online at http://www.cell.com/cgi/content/full/115/2/209/DC1).

The differential internal stability profiles were then compared between functional and nonfunctional subgroups of the whole siRNA panel consisting of 217 members. When the average difference between 5′-AS and 5′-S values were plotted for both functional and nonfunctional subgroups, it became clear that (on average) the 5′ AS region is less stable than the 5′ S terminus in functional siRNAs and that an opposite trend (i.e., the 5′-S end is more stable than 5′ AS) was characteristic of nonfunctional molecules (Figure 2C). As the calculated p value is 0.0123 (standard t-test), the observed distribution is nonrandom and likely identifies a critical parameter in siRNA processing, possibly predefining the selective strand entry into the RISC complex.

In addition to the termini, major stability differences are observed at other positions within the duplex of functional and nonfunctional siRNA. At positions 9–14 (counting from the 5′-AS end), the functional siRNA subset is enriched with molecules that have low internal stability (Figure 2B). In contrast, the nonfunctional subset is enriched with members that have high internal stability in this region. On average, the differential stability of the two sets in this region is $\Delta G \sim 1.6$ kcal/mol and significant. We hypothesize that because the target mRNA is cleaved between position 9 and 10 from the 5′ end of the anti-sense strand, additional flexibility in this region might be important for target cleavage and/or release of the products upon the cleavage by the RISC-associated endonuclease, leading to the regeneration of RISC*.

The observed trend in functional siRNA stability profiles suggests that these thermodynamic features play an important role in RNA interference, possibly promoting efficient entry and recognition by RISC. A logical extension of this hypothesis is that siRNA molecules lacking these properties would be selected against and eventually degraded in an RNase-rich intracellular environment. If this were the case, one would predict that after introduction of long dsRNAs into a cell's cytoplasm, only those siRNAs that share the predescribed profile of functional siRNA would survive and be identified at later times. Moreover, one would further speculate that

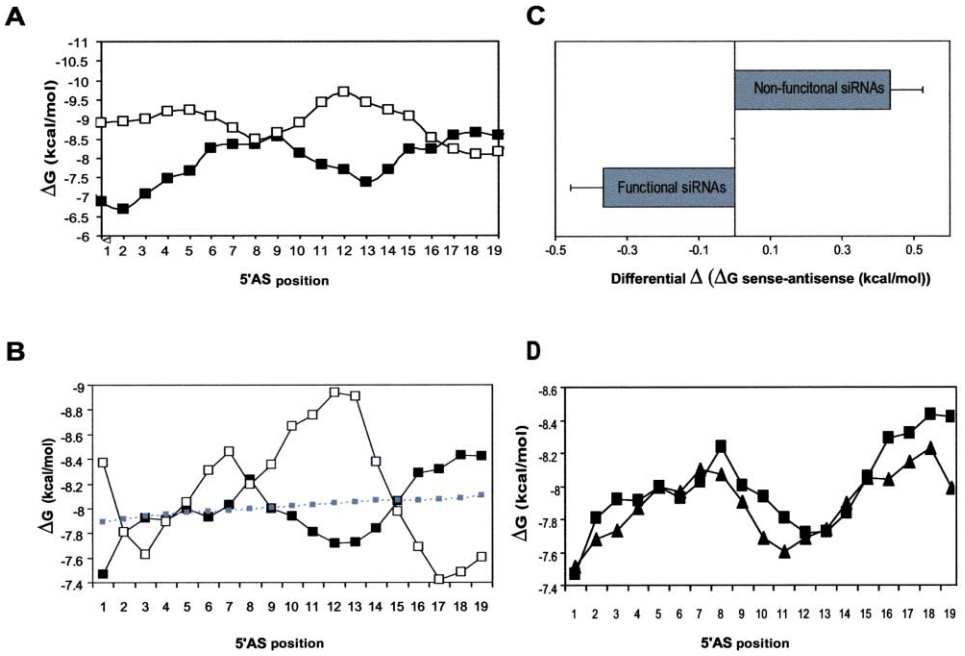

Figure 2. Characterization of the siRNAs Internal Stability Profile

(A) Calculated average internal stability profiles for a set of 37 siRNAs targeting human and mouse genes (functional siRNAs, ■, sample size of 16; and nonfunctional siRNAs, □, sample size of 21).

(B) Calculated average internal stability profiles for a set of 180 siRNAs targeting every other position of firefly luciferase and human cyclophilin (functional siRNAs, ■, sample size of 53; nonfunctional siRNAs, □, sample size of 41; the complete siRNA panel, ■, sample size of 180).

(C) Calculated differential average internal stability of 5′ S and 5′ AS end of 180 siRNA duplexes for functional and nonfunctional subsets (5′ S–5′ AS).

(D) Calculated average internal stability profiles for a set of 59 GFP-related siRNAs identified by cloning after introduction of the long double-stranded GPF RNA into the plant cells (GFP related siRNAs, ▲; functional siRNAs from the 180 siRNA panel, ■).

it is the profile that determines whether an siRNA is retained rather than the functionality of the molecule. Thus, siRNA having the proper profile on either the sense or anti-sense strand should be preserved if the key factor for intracellular retention is the thermodynamic profile and not the presence of the mRNA target sequence. To address this question, we analyzed the internal stability profiles of siRNA molecules generated by introduction of long dsRNAs into *Nicotiana benthamiana*. Specifically, in work described by Llave et al. (2002), plant leaves were infiltrated with *Agrobacterium tumefaciens* containing expression cassettes for transcripts corresponding to the intron-spliced, inverted-repeat form of the GFP sequence. Subsequently, 59 short, double-stranded RNAs having homology to GFP were reisolated from the plant tissue. We determined the AISP values for all 59 sequences. The data were then examined, ignoring the conventions of sense and anti-sense polarity, and averaged to generate a single profile for the entire family that could be compared with the AISP of functional siRNA. As shown in Figure 2D when the data were analyzed by these means, the profile of surviving GFP siRNA traces the pattern observed in previously studied, functional siRNA. The 5′ terminus exhibits heightened instability compared to the 3′ terminus, and the region between 9–14 demonstrates additional flexibility compared to the rest of the molecule. It should be emphasized that in this analysis, ~50% of surviving siRNAs were aligned with the sense strand (relative to the GFP sequence), thus suggesting that siRNAs with the functional profiles are retained independently of the presence or absence of a target mRNAs. Together, these data demonstrate that (1) the low internal stability of the 5′ terminus of the anti-sense strand, as well as a decreased thermodynamic stability in the region of 10–14, appear to be a common feature shared by both functional siRNAs and naturally occurring precursor/mature miRNAs found in different organisms, and (2) that natural selection of siRNA is not based solely on function but, rather, surviving siRNAs are retained on the basis of the thermodynamic properties of the molecule.

Specific Thermodynamic Profiles of siRNA Correlate Well with the Functionality

Given that siRNAs and miRNAs share common internal stability signatures, we extended the analysis to assess whether these features, present individually or together, could be useful for predicting silencing efficiency. To evaluate the putative role of the 5′-AS end instability in silencing, ten siRNAs targeting human secreted alkaline phosphatase (SEAP; NM_001632) were randomly designed disregarding their thermodynamic properties, and their activity was assessed in HEK293 cells cotransfected with a SEAP reporter (Figure 3A). Of the ten siRNAs (SEAP-68, -147, -155, -206, -500, -812, -923, -1113, -1117, and -1271), three induced 70% or greater reduction in SEAP expression while seven siRNAs were considered inactive or inefficient with less than 70% target

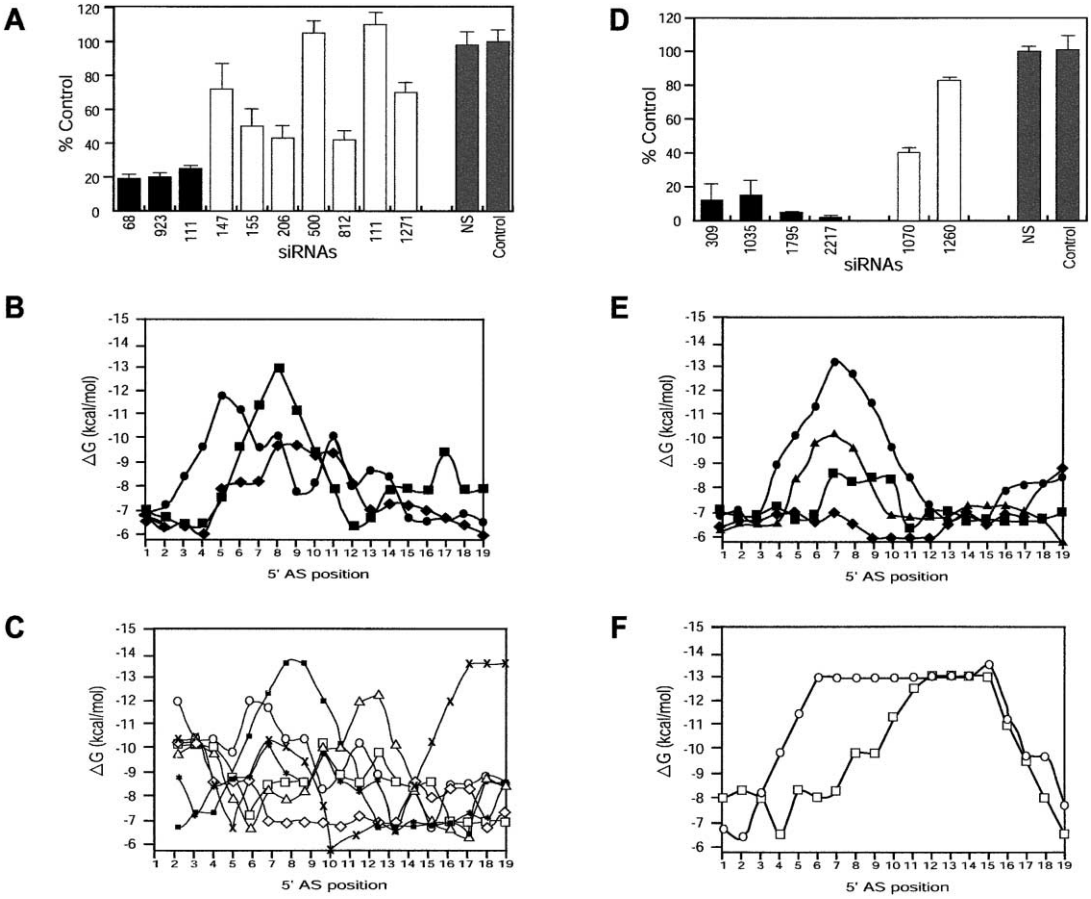

Figure 3. Thermodynamic and Functional Characterization of siRNA Duplexes Targeting Human SEAP

(A) Gene silencing of SEAP associated with siRNAs designed without regard for thermodynamic signatures. Functional siRNAs SEAP-68, -923, and -1117 (black bars); nonfunctional siRNA SEAP-147, -155, -206, -500, 812, -1113, and -1271 (open bars); nonspecific sequence control (NS, gray bar); and nontransfected control (gray bars).

(B) The internal stability profiles of functional siRNAs in (A). Shown are SEAP-68 (■), SEAP-923 (◆), and SEAP-1117 (●).

(C) The internal stability profiles of nonfunctional siRNAs in (A). Shown are SEAP-147 (□), -155 (◇), -206 (■), -500 (□), -812 (*), -1113 (△), and –1271(X).

(D) Reduction of SEAP associated with siRNAs designed to satisfy zero, one, or both of the thermodynamic signatures. Functional siRNAs SEAP-309, -1035 -1795 and - 2217 (filled bars), nonfunctional siRNA SEAP-1070 and -1260 (open bar), nonspecific sequence control (NS, gray bar), and nontransfected control (gray bar).

(E) The internal stability profiles of functional siRNAs in (D). Shown are SEAP-309 (▲), -1035 (■), -1795 (●), and -2217 (◆).

(F) The internal stability profiles of nonfunctional siRNAs in (D). Shown are SEAP-1070 (□) and -1260 (○).

reduction (Figure 3A). Figures 3B and 3C illustrate the internal stability profiles calculated for the functional and nonfunctional siRNAs. As expected, all three functional siRNAs exhibited a low internal stability profile of the 5′-AS strand, especially at the terminal position, consistent with the characteristic profile observed for miRNAs. Among the seven nonfunctional duplexes, six had highly stable 5′-AS ends matched with a highly variable internal stability profile throughout the rest of the molecule. Interestingly, one of the nonfunctional siRNAs (SP-206) exhibited relatively low internal stability at the 5′ AS terminus but reduced SEAP expression by only 51% (Figure 3C; gray squares). This finding indicates that low internal strand stability at the 5′-AS end is important for activity, but other factors likely contribute to siRNA functionality.

Next, several siRNAs containing acceptable thermodynamic signatures were identified. Specifically, all four siRNAs (SEAP-309, -1035, -1795, and -217) contained a low internal stability at the 5′-AS terminal position and exhibited an average internal stability at positions 9–14 that was lower than −8.5 kcal/mol. In addition, to determine whether the low internal stability at the 5′−AS end was sufficient to confer functionality, two additional siRNAs (SEAP-1070 and SEAP-1260) were synthesized. SEAP-1070 has an internal stability of approximately −13 kcal/mol at the 9–14 nt region, a value that is high compared to the miRNAs and functional siRNAs studied thus far. However, the 5′-AS terminal internal stability of SEAP-1070 was low (−6.5 kcal/mol), thus enabling distinction between the contributions made by the 9–14 region and the 5′ AS. In contrast, SEAP-1260 has high internal stability at both the 5′ AS and region 10–14 and should, according to our predictions, be nonfunctional. As shown in Figure 3D, all four of the siRNAs designed to satisfy both thermodynamic signatures were functional,

reducing SEAP protein expression by more than 85%. In contrast, both SEAP-1070 and SEAP-1260, siRNAs that lacked conformity at either the 9–14 nt region or the 5′-AS position and the 9–14 nt region, induced less than 70% gene silencing.

These results indicate that the enhanced flexibility at the 5′-AS terminal position and the low internal energy across the duplex (especially at the region 9–14) are strongly correlated with siRNA function. However, it is also evident that while these properties may be required, they are not sufficient for silencing activity (as suggested by the single outlier found within the ten randomly selected SEAP siRNAs). Evaluation of the thermodynamic stability alone for this nonfunctional siRNA would have predicted it to be functional.

Mechanistic Implications

Here, we have identified a thermodynamic signature that is common amongst most miRNA precursors and functional siRNAs. Specifically, both classes of molecules exhibit enhanced flexibility at the 5′ AS terminus and an overall low internal stability profile, in particular within the 9–14 bp region of the duplex. Using this thermodynamic signature, we have scanned gene sequences and identified multiple regions with similar patterns. Cell-based tests of siRNAs designed from these regions have shown them to be potent agents of gene silencing, thus suggesting that identification of specific thermodynamic profiles might be useful tool in the search for functional siRNA. Moreover, altering the chemical or structural nature of the siRNA duplex (introducing mismatches and chemical modifications), which will alter the internal stability profiles to resemble the desirable one, might be a means for optimization of siRNA activity.

The apparent differential internal stability signature of functionally active siRNAs/miRNAs is likely to play an important role in several steps of the RNAi pathway, including duplex unwinding, strand selection, and product release. For unwinding to occur efficiently, double-stranded duplexes need to be destabilized either by structural elements inherent in the sequence or by low internal stability of the sequence itself. In miRNAs, these destabilizing elements come in the form of base pair mismatches, gaps, and bulges. In contrast, in siRNAs either generated naturally from long double-stranded RNAs or obtained synthetically, such structural elements do not exist, thus prompting the need of other factors to reduce the internal stability at key positions within the molecule.

Initially, siRNAs form a precomplex with RISC components. A priori, such precomplexes could form at either terminus (5′ S or 5′ AS) with an equal probability to initiate unwinding of the duplex by a helix associated with RISC (Figure 4). If the 5′ AS terminus has enhanced flexibility, as in miRNAs and functional siRNAs, it is likely that helicase activity would be biased toward unwinding the more unstable 5′ AS terminus. As the two strands unwind, RISC has the ability to keep either strand associated with it. As shown here, thermodynamic profiles of miRNAs and siRNAs isolated from plant cells revealed that the strand having the low internal stability at the 5′ end is retained within the RISC. It has also been demonstrated that for effective RNA interference to occur, a 5′-phosphate group must be present on the AS strand (Martinez et al., 2002; Nykanen et al., 2001). The biased asymmetric opening of the siRNA molecule by RISC may enable strand selectivity, possibly through interactions with newly freed 5′ phosphate on the antisense strand. Alternatively, the RISC may choose the strand based on backbone polarity: 5′→3′, as opposed to 3′→5′. Thus, the bias in the thermodynamic profile would eventually determine which end of the molecule is selected for preferential unwinding and which strand will be retained by RISC. Indeed, it has been demonstrated in in vitro studies that both the absolute and relative stabilities of the base pairs at the 5′ ends of the two siRNA strands determines the degree to which each strand participates in the RNAi pathway (Schwarz et al., 2003).

The fundamental importance of the substrate internal stability may suggest that the hypothetical RISC-associated helicase belongs to the DEAD box family of helicases in which ATP-dependent unwinding of an initial 4–5 bp region is followed by helicase dissociation and then reassociation at the next 4–5 bp interval (Nykanen et al., 2001). When the internal stability of the terminal pentameric sequence of the 5′ AS strand is high, rewinding would occur rapidly and prevent unwinding.

Studies of siRNA, derived from the introduction of long dsRNA into *Nicotiana benthamiana*, provided insights into the parameters used by nature to select siRNAs. The thermodynamic profile of the 59 molecules isolated from plants infected with long dsRNA shows conformity with the signature identified in functional siRNA molecules. Interestingly, half of these siRNAs retained sense polarity to the target mRNA, indicating that their siRNA duplexes had less stable 5′ S termini. Not only does this observation validate the importance of using thermodynamic signatures to identify RISC substrates, but it also further implies that it is the thermodynamic profile of the molecule and not the functionality of the siRNA per se that determines whether it will be preserved within a cell.

Once RISC* is formed, it should have multiple turnover of the target to have effective gene silencing, an event that requires the dissociation of the target molecule after cleavage at a position opposite the center of the antisense "guide." The observed low overall internal stability of functional siRNAs, especially spanning the cleavage region (9–14 nt) may facilitate product release, thus allowing the RISC* to find a second substrate. Alternatively, flexibility in this region may play a critical role in RISC complex function, specifically enabling the most favorable conformation during mRNA cleavage.

As has been demonstrated (Jackson et al., 2003; Saxena et al., 2003), intracellular siRNA activity may not be as specific as it was originally thought. One of the possible contributions for "off-target" effects may stem from the sense strand entering into the RISC, which could be potentially blocked by choosing siRNAs with high internal stability at the 5′ end of the sense strand or by chemical modifications of this end to prevent RISC association (e.g., capping the 5′ end of the sense strand to prevent intracellular phosphorylation). Detailed understanding of the molecular mechanism of RNAi as well as the nature of the key protein players and their specific roles within the RISC would expect to reveal possible

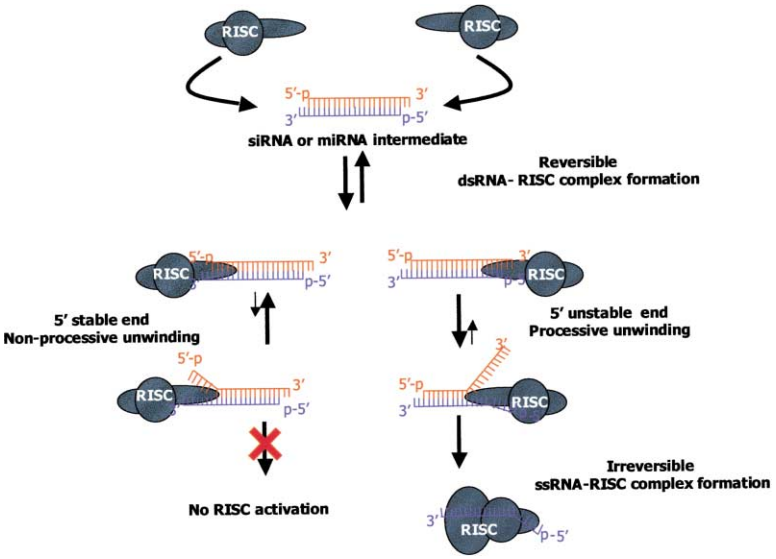

Figure 4. A Proposed Model for How the Thermodynamic Characteristics within an siRNA or miRNA Contribute to Efficient RNAi

A protein ensemble that constitutes RISC forms reversible complexes with either 5′ end of the siRNA or miRNA duplex. The enhanced flexibility of the 5′ AS terminus facilitates the directional unwinding of the duplex from the 5′ AS end to promote the formation of the more stable activated RISC*. In this way, differential stability of the two ends of the siRNA or miRNA duplex predetermines which strand is selectively loaded into the RISC*.

approaches for curbing off-target effects observed in siRNA-mediated gene silencing.

In conclusion, the analysis performed on miRNA precursors, functional siRNAs, and siRNAs selectively surviving in cells after introduction of long dsRNAs revealed specific thermodynamic signatures that are favorable for RNA interference. The similarity in the thermodynamic signatures between siRNAs and miRNAs further support the view that both miRNAs and siRNAs share common pathways and protein machinery. Future studies dedicated toward understanding the biophysical properties involved in RNAi will lead to the development of improved predictive models for selecting functional siRNAs.

Experimental Procedures

siRNA Preparation

siRNAs against firefly luciferase and human cyclophilin were designed to target every other position of the following regions. Human cyclophilin: 193–390, M60857, GTTCCAAAAACAGTGGATAATTTTG TGGCCTTAGCTACAGGAGAGAAAGGATTTGGCTACAAAAACAGC AAATTCCATCGTGTAATCAAGGACTTCATGATCCAGGGCGGAGA CTTCACCAGGGGAGATGGCACAGGAGGAAAGAGCATCTACGGT GAGCGCTTCCCCGATGAGAACTTCAAACTGAAGCACTACGGGCC TGGCTGGG; firefly luciferase: 1434–1631, U47298 (pGL3, Promega), TGAACTTCCCGCCGCCGTTGTTGTTTTGGAGCACGGAAAGACGA TGACGGAAAAAGAGATCGTGGATTACGTCGCCAGTCAAGTAACA ACCGCGAAAAAGTTGCGCGGAGGAGTTGTGTTTGTGGACGAAGT ACCGAAAGGTCTTACCGGAAAACTCGACGCAAGAAAAATCAGAG AGATCCTCATAAAGGCCAAGAAGG.

siRNAs targeting the following positions of the fLuc: 15, 21, 35, 39, 45, 49, 51, 61, 63, 65, 67, 77, 79, 97, 99, 105, 107, 109, 111, 113, 115, 125, 127, 133, 135, 139, 143, 145, 147, 149, 151, 153, 155, 157, 159, 161, 167, 169, 171, and 173; and human cyclophilin: 5, 27, 35, 41, 43, 45, 65, 69, 95, 99, 131, 139, and 159 induced more then 90% gene silencing; siRNAs targeting the following positions of the fLuc: 3, 7, 11, 17, 23, 25, 29, 31, 59, 71, 85, 87, 89, 91, 95, 101, 117, 119, 175, and 179; and human cyclophilin: 7, 9, 11, 17, 23, 31, 51, 61, 63, 73, 97, 101, 103, 113, 115, 119, 149, 151, 171, 173, and 179 induced less then 50% gene silencing (A.R., D. Leake, K. Boese, M. Marshall, S. Scaringe, and A.K., unpublished data).

siRNA targeting sites in human SEAP: were as follows. SP-68, 5′-CAGAAGTCCGGGTTCTCCT; SP-147, 5′-TCTGGTGCAGGAATGG CTG; SP-155, 5′-ACCTCATCATCTTCCTGGG; SP-309, 5′-ACTGTC TGGCACATGTTTG; SP-500, 5′-GGCGAGGCGTGCTGCACTC; SP-812, 5′-GAATCTGGTGCAGGAATGG; SP-923, 5′-CTTTGAGCCTGG AGACATG; SP-1035, 5′-GAACATGATCGTCTCAGTC; SP-1070, 5′-AACATCCGGCCGGGCGCCG; SP-1070, 5′-CTGGTGAGCTGGCCC GCCC; SP-1113, 5′-GTGGGAGTGGTCGGCAGTG; SP-1117, 5′-TGTTCGACGACGCCATTGA; SP-1271, 5′-CGGATGTTACCGAGAG CGA; SP-1795, 5′-TGACAACGGGCCACAACTC; SP-2217, 5′-ACTC TCTGACATACATCAC.

All duplexes were synthesized at Dharmacon as 21-mers with dTdT 3′ overhangs using a modified method of 2′-ACE chemistry (Scaringe, 2000). siRNA strands were annealed in a buffer consisting of 100 mM KCl, 30 mM HEPES (pH 7.5), and 2 mM $MgCl_2$ by heating to 90°C for 2 min, followed by slow cooling to ambient temperature.

Evaluation of siRNA Activity in Tissue Culture

Cell lines expressing the target of interest (HEK293, Calu-6, MDA-75, or HEK-293-Luc) were obtained from ATCC (Manassas, VA) and grown to 70%–80% confluency in 96-well plates. siRNAs (at 100 nM final concentration) were transfected with Lipofectamine 2000 (Invitrogen) according to the manufacturer's instructions. For the cotransfection experiments, the plasmid expressing the SEAP reporter (pAAV6, an adeno-associated vector containing the human SEAP gene upstream of the 3′-untranslated region (3′-UTR) of bovine growth hormone) was used at 0.25 μg/ml concentration. Cells were grown for 24 hr in a 37°C incubator with 5% CO_2. Target mRNA levels were quantified by branched DNA (bDNA) technology (Collins et al., 1997) using the QuantiGene High Volume Kit (Bayer) and target specific probes according to the manufacturer's instructions. SEAP levels were measured using the Great EscAPe SEAP assay (Clontech). Firefly luciferase levels were measured using the SteadyGlo assay (Promega). Data were normalized to the level of cyclophilin or GAPDH and measured by bDNA. No cytotoxicity was observed in any of the reported experiments as measured by Alamar Blue (Trek Diagnostic Systems). Each data point represents an average of three independent experiments, with error bars representing the standard deviation from the average.

The Oligo 5.0 Primer Analysis Software (National Biosciences, Inc., Plymouth, MN) was used for calculations of internal stability profiles using the free energy values in Table 1 (−kcal/mol, adjusted to 25°C).

In general, sequences were downloaded into Oligo 5.0, and the output was transferred to an Excel spreadsheet. The internal stability values reflect the stability of pentamer subsequences within the sequence under investigation and were calculated according to the nearest neighbor method (Freier et al., 1986). For the calculation of the average internal stability values of the terminal four bases on the 3′ end of the molecule, the 19 bp targeting sites were extended based on the target mRNA or miRNA precursor sequences.

No initiation ΔG value was included in calculations. To simplify

calculations, the internal stability values were first calculated for the perfect duplex, and the gap penalty (set at −2.1 kcal/mol) and mismatch penalties were included wherever necessary. Mismatch (mm) penalties varied on the nature of the eliminated base pair and were calculated according to the nearest neighbor rules. For example, the mm penalty for the G/a mm in a context of the adjacent GC base pair will be 2.7 kcal/mol and the mm penalty for the A/g mm in a context of the adjacent AU base pair will be 1.1 kcal/mol.

Acknowledgments

We thank Alexey Wolfson, Sid Suggs, and Bill Marshall for helpful discussions; Phillip Zamore sharing data prior to publication; Julie Ross-Kramer and Stephanie Hartsel for oligo synthesis; and Jon Karpilow and Queta Boese for help with manuscript preparation.

Received: June 30, 2003
Revised: September 18, 2003
Accepted: September 22, 2003
Published: October 16, 2003

References

Ambros, V., Bartel, B., Bartel, D.P., Burge, C.B., Carrington, J.C., Chen, X., Dreyfuss, G., Eddy, S.R., Griffiths-Jones, S., Marshall, M., et al. (2003). A uniform system for microRNA annotation. RNA *9*, 277–279.

Bernstein, E., Caudy, A.A., Hammond, S.M., and Hannon, G.J. (2001). Role for a bidentate ribonuclease in the initiation step of RNA interference. Nature *409*, 363–366.

Collins, M.L., Irvine, B., Tyner, D., Fine, E., Zayati, C., Chang, C., Horn, T., Ahle, D., Detmer, J., Shen, L.P., et al. (1997). A branched DNA signal amplification assay for quantification of nucleic acid targets below 100 molecules/ml. Nucleic Acids Res. *25*, 2979–2984.

Doench, J.G., Petersen, C.P., and Sharp, P.A. (2003). siRNAs can function as miRNAs. Genes Dev. *17*, 438–442.

Elbashir, S.M., Harborth, J., Lendeckel, W., Yalcin, A., Weber, K., and Tuschl, T. (2001a). Duplexes of 21-nucleotide RNAs mediate RNA interference in cultured mammalian cells. Nature *411*, 494–498.

Elbashir, S.M., Lendeckel, W., and Tuschl, T. (2001b). RNA interference is mediated by 21- and 22-nucleotide RNAs. Genes Dev. *15*, 188–200.

Elbashir, S.M., Harborth, J., Weber, K., and Tuschl, T. (2002). Analysis of gene function in somatic mammalian cells using small interfering RNAs. Methods *26*, 199–213.

Fire, A., Xu, S., Montgomery, M.K., Kostas, S.A., Driver, S.E., and Mello, C.C. (1998). Potent and specific genetic interference by double-stranded RNA in Caenorhabditis elegans. Nature *391*, 806–811.

Freier, S.M., Kierzek, R., Jaeger, J.A., Sugimoto, N., Caruthers, M.H., Neilson, T., and Turner, D.H. (1986). Improved free-energy parameters for predictions of RNA duplex stability. Proc. Natl. Acad. Sci. USA *83*, 9373–9377.

Grishok, A., Pasquinelli, A.E., Conte, D., Li, N., Parrish, S., Ha, I., Baillie, D.L., Fire, A., Ruvkun, G., and Mello, C.C. (2001). Genes and mechanisms related to RNA interference regulate expression of the small temporal RNAs that control C. elegans developmental timing. Cell *106*, 23–34.

Hammond, S.M., Bernstein, E., Beach, D., and Hannon, G.J. (2000). An RNA-directed nuclease mediates post-transcriptional gene silencing in Drosophila cells. Nature *404*, 293–296.

Hutvágner, G., McLachlan, J., Pasquinelli, A.E., Balint, E., Tuschl, T., and Zamore, P.D. (2001). A cellular function for the RNA-interference enzyme Dicer in the maturation of the let-7 small temporal RNA. Science *293*, 834–838.

Hutvágner, G., and Zamore, P.D. (2002). A microRNA in a multiple-turnover RNAi enzyme complex. Science *297*, 2056–2060.

Jackson, A., Bartz, S.R., Schelter, J., Kobayashi, S.V., Burchard, J., Mao, M., Li, B., Cavet, G., and Linsley, P.S. (2003). Expression profiling reveals off-target gene regulation by RNAi. Nat. Biotechnol. *21*, 635–637.

Ketting, R.F., Fischer, S.E., Bernstein, E., Sijen, T., Hannon, G.J., and Plasterk, R.H. (2001). Dicer functions in RNA interference and in synthesis of small RNA involved in developmental timing in C. elegans. Genes Dev. *15*, 2654–2659.

Largos-Quintana, M., Rauhut, R., Lendeckel, W., and Tuschl, T. (2001). Identification of novel genes coding for small expressed RNAs. Science *294*, 853–858.

Lau, N.C., Lim, L.P., Weinstein, E.G., and Bartel, D.P. (2001). An abundant class of tiny RNAs with probable regulatory roles in Caenorhabditis elegans. Science *294*, 858–862.

Lee, R.C., and Ambros, V. (2001). An extensive class of small RNAs in Caenorhabditis elegans. Science *294*, 862–864.

Llave, C., Kasschau, K.D., Rector, M.A., and Carrington, J.C. (2002). Endogenous and silencing-associated small RNAs in plants. Plant Cell *14*, 1605–1619.

Martinez, J., Patkaniowska, A., Urlaub, H., Luhrmann, R., and Tuschl, T. (2002). Single-stranded antisense siRNAs guide target RNA cleavage in RNAi. Cell *110*, 563–574.

Mourelatos, Z., Dostie, J., Paushkin, S., Sharma, A., Charroux, B., Abel, L., Rappsilber, J., Mann, M., and Dreyfuss, G. (2002). miRNPs: a novel class of ribonucleoproteins containing numerous microRNAs. Genes Dev. *16*, 720–728.

Nicholson, R.H., and Nicholson, A.W. (2002). Molecular characterization of a mouse cDNA encoding Dicer, a ribonuclease III ortholog involved in RNA interference. Mamm. Genome *13*, 67–73.

Nykanen, A., Haley, B., and Zamore, P.D. (2001). ATP requirements and small interfering RNA structure in the RNA interference pathway. Cell *107*, 309–321.

Plasterk, R.H. (2002). RNA silencing: the genome's immune system. Science *296*, 1263–1265.

Saxena, S., Josson, Z.O., and Dutta, A. (2003). Small RNAs with imperfect match to endogenous mRNA repress translation: implications for off-target activity of siRNA in mammalian cells. J. Biol. Chem., in press. Published online September 2, 2003. 10.1074/jbc.M307089200.

Scaringe, S.A. (2000). Advanced 5′-silyl-2′-orthoester approach to RNA oligonucleotide synthesis. Methods Enzymol. *317*, 3–18.

Schwarz, D.S., Hutvágner, G., Du, T., Xu, Z., Aronin, N., and Zamore, P.D. (2003). Asymmetry in the assembly of the RNAi enzyme complex. Cell *115*, this issue, 199–208.

Zamore, P.D., Tuschl, T., Sharp, P.A., and Bartel, D.P. (2000). RNAi: double-stranded RNA directs the ATP-dependent cleavage of mRNA at 21 to 23 nucleotide intervals. Cell *101*, 25–33.

Zeng, Y., Yi, R., and Cullen, B.R. (2003). MicroRNAs and small interfering RNAs can inhibit mRNA expression by similar mechanisms. Proc. Natl. Acad. Sci. USA *100*, 9779–9784.